Time-Resolved Fourier Transform Infrared Emission Spectroscopy of CO $\Delta v = 1$ and $\Delta v = 2$ Extended Bands in the Ground $X^1\Sigma^+$ State Produced by Formamide Glow Discharge

Adam Pastorek[1,2], Svatopluk Civiš[1,*], Victoria H.J. Clark[3], Sergei N. Yurchenko[3], Martin Ferus[1]

1 – J. Heyrovsky Institute of Physical Chemistry, Czech Academy of Sciences, Dolejškova 2155/3, 18200, Prague 8, Czech Republic
2 – Faculty of Nuclear Sciences and Physical Engineering, Czech Technical University in Prague, Břehová 78/7, 11519, Prague 1, Czech Republic
3 – Faculty of Mathematical and Physical Sciences, University College London, Gower Street, London WC1E 6BT, United Kingdom

** Corresponding author*

Abstract

This paper presents an extension to our knowledge of $\Delta v = 1$ and $\Delta v = 2$ bands of carbon monoxide in the ground state, measured by Fourier transform infrared spectroscopy of glow discharge of formamide-nitrogen mixture. Lines in declared bands are measured up to $v = 30$ for $\Delta v = 1$ and up to $v = 24$ for $\Delta v = 2$ band, by use of both InSb and MCT detectors, which have not been measured in the laboratory before. Dunham parameters obtained by fitting our lines are presented as well as comparison to other authors. The paper also demonstrates the interesting impossibility of sufficient population of $\Delta v = 2$ band of CO when only pure CO is used in the glow discharge, instead of formamide-based mixture. Additionally, we present a non-LTE model to describe the intensity pattern of the $\Delta v = 1$ and the $\Delta v = 2$ bands of $^{12}C^{16}O$ experimental spectra by simulating the corresponding non-LTE vibrational populations of CO.

Keywords

Spectroscopy, carbon monoxide, glow discharge, time resolved, FTIR, formamide

Competing interests statement

Authors declare no conflicts of interest.

Introduction

There have been attempts to measure the full range of fundamental ($\Delta v = 1$) and first overtone ($\Delta v = 2$) bands of CO since the very beginnings of Fourier spectroscopy.[1–3] CO, as an important molecule, can be found not only on Earth but also in interstellar space.[4] Here the spectroscopy can serve as a tool for determining the isotopic ratios of C and O,[5,6] thus providing more information about the evolution of stars etc. CO is the most stable diatomic molecule and is the second most abundant specie (after hydrogen) in cool interstellar sources.[7] In the Earth's atmosphere, carbon monoxide is a spatially variable molecule (about 80 ppb) and a short-lived specie (about 3 months in the troposphere), having a role in the formation of ground level ozone. This chemical compound is an important component of the exhaust from the incomplete combustion of fuels containing carbon and its compounds under various conditions. Beyond this planet, CO has been detected in the solar photosphere, atmospheres of planets, in the spectra of stars and interstellar clouds.[8] Its first spectral detection in absorption regime in the mid-infrared region took place in 1889, when CO became the first diatomic compound measured in the gaseous phase for which such observations were made.[9]

The rotation-vibration lines of the carbon monoxide molecule are commonly used in the laboratory as a wavelength standard for calibration of infrared instruments.[10,11] Spectral measurements played a dominant role in monitoring CO presence under different conditions. While the detection of CO in several isotopic variants in the microwave spectral region is preferable for distant astronomical objects, the infrared observation becomes more favourable for monitoring of exhaust fumes from stationary or mobile burners, or radiation from lasers or comparable gaseous plasma systems. Accurate knowledge of frequencies and intensity of spectral transitions is essential for all such monitoring.

One of the first multi-isotopic determinations of the mass-independent Dunham coefficients (U_{mj} and Δ_{mj}) of the CO molecule was made by George *et al.*[12] They used highly accurate microwave and infrared heterodyne frequency measurements. Obtained fitted values allow the reproduction of almost all measured frequencies within the measured uncertainties. Previously, Farrenq *et al.*[13] used the most extensive set of measured frequencies to determine the precise set of Dunham coefficients. The dataset included transition frequencies coming from both laboratory and solar Fourier spectra of seven isotopes of CO up to $J_{max} = 133$ and $v_{max} = 41$.

Alongside the aforementioned publications, other experimental or theoretical high precision data for various CO isotopes[14–28] or CO-related research have been published.[29–35]

Critical evaluation of measured pure-rotation and rotation-vibration line positions and an experimental dataset of energy levels of $^{12}C^{16}O$ in $X^1\Sigma^+$ state was carried out by Tashkun[36] and by T.I. Velichko.[37] All available transitions from microwave to visible region (3.8 –10 440 cm^{-1}) of the $^{12}C^{16}O$ molecule were collected from the literature and tested using the RITZ computer code. These data have been critically analysed and used to obtain the most complete and precise set of 2247 experimental energy levels of this molecule covering 0-67 000 cm^{-1} interval.

The numerous $^{12}C^{16}O$ transitions of overtone bands have been reported by A.P. Mishra,[38] Malathy Devi,[39] ($\Delta v = 2$ sequence) and also Picqué[40] and Swann,[41] who published new data for the $\Delta v = 3$ band. The results of Ogilvie *et al.*[9] are related to the identification of the $\Delta v = 4$ band and Chung's *et al*.[42] data for the $\Delta v = 5$ band are also available now.

There is still a small gap for the high resolution infrared measurement of weak rovibrational spectral lines, especially for the highly vibrationally excited spectral bands concerning $\Delta v = 1$ and $\Delta v = 2$ bands. The turning point here is the application of time resolved high resolution infrared Fourier transform formamide emission discharge measurement, followed by detailed analysis of time resolved emission spectra containing mainly spectra of highly excited molecules of CO and CN radical together. The method of time resolved measurement enables the distinguishing of weak emission (or absorption) bands from strong bands appearing in the spectrum inside of the time-profiles spectra. In the case of CN, weak vibronic bands in the 5 μm region were separated from strong long lived vibration–rotation bands.[43]

Normally, experimental spectra of molecules are recorded at local thermal equilibrium (LTE), i.e. ro-vibrational populations satisfy, and are limited by, the Boltzmann distribution at the corresponding well temperatures. The so-called non-LTE spectroscopy allows one to decouple the rotational and vibrational degrees of freedom from each other and, most importantly, from the lab temperature (e.g. Dudás *et al.* 2020).[44] For example, reducing the rotational temperature leads to less crowded spectra and facilitates analysis, while increasing the vibrational temperatures helps to involve highly excited vibrational states, which are otherwise switched off owing to the lack of the thermal populations.[44] The discharge experimental techniques have proved to be efficient in providing spectra of hot, non-LTE excitations of vibrational states.[45–47]

The modelling of the molecular non-LTE spectra is not trivial. A typical non-LTE model is to represent the rovibrational population using a two-temperature Boltzmann distribution with rotational and vibrational states described by the corresponding LTE distributions (Treanor distribution).[48] As was shown previously,[48] the Treanor distribution typically breaks for the spectra of products of complex discharged species, where their vibrational populations do not satisfy the simple Boltzmann law (e.g. as shown for N_2;[49] CO[50,51] and CO_2[52]). Numerous models exist in the literature for dissociative and recombination processes leading to the non-LTE spectral distributions, see e.g. Ferus *et al.* (2017)[47] & references within.[50,53]

In this paper we report a spectroscopic analysis of more than 200 newly observed $^{12}C^{16}O$ first overtone transitions located between v = 18-24 (measured from discharge plasma emission of formamide, compared to Mishra *et al.*[38]), including a new fitted set of Dunham coefficients. The transitions involve J values up to 30 and reaching v = 24. We also extend the experimentally observed CO fundamental band to v = 30, which is more than e. g. Farrenq *et al.*[13] reported in their measurement of solar spectra; it has to be noted, however, Farrenq reached extremely high J numbers, due to very hot spectral source (Sun). We also present a robust method for estimating non-LTE vibrational populations for description of the CO intensities produced in the discharging of the formamide molecule from the experimental study in Ferus *et al.* (2014).[46] Our model is based on 1D harmonic populations to describe the CO fragment created from a dissociating formamide molecule and of the free CO molecule and on the usage of accurate synthetic line list for CO.[54,55] The methodology can be applied for the description of non-LTE spectra of other products of formamide and will be published elsewhere.

Experimental arrangement

For the measurement of emission bands of CO, Bruker IFS 120 HR time-resolved spectrometer has been used. The entry window of the spectrometer was from CaF_2, as well as the inner beam-splitter and discharge cell window; when InSb liquid nitrogen cooled semiconductor detector was used. In the case of MCT detector, KBr entry and cell windows together with KBr beam-splitter were used. Entry aperture of the spectrometer was 1.7 mm. The pre-discharge mixture was consisting of vapours of formamide (CAS 75-12-7, Sigma-Aldrich) mixed with gaseous nitrogen and water at 60 °C. The mixture was continuously injected in the discharge of pure helium at 1.8 torr of pressure. The pressure of the resulting mixture in the discharge cell was peaking ~ 2 torr and the whole system was in a continuous flow maintained by vacuum rotary pump to ensure a proper exhaust discharge. The voltage of the glow discharge was 1 kV and the electric current was 0.1 mA. The spectrometer was evacuated to 10^{-3} mbar. The spectra were recorded in a 0.02 cm^{-1} resolution, with averaging over 200 scans. Data were processed by Norton-Beer weak apodization algorithm.

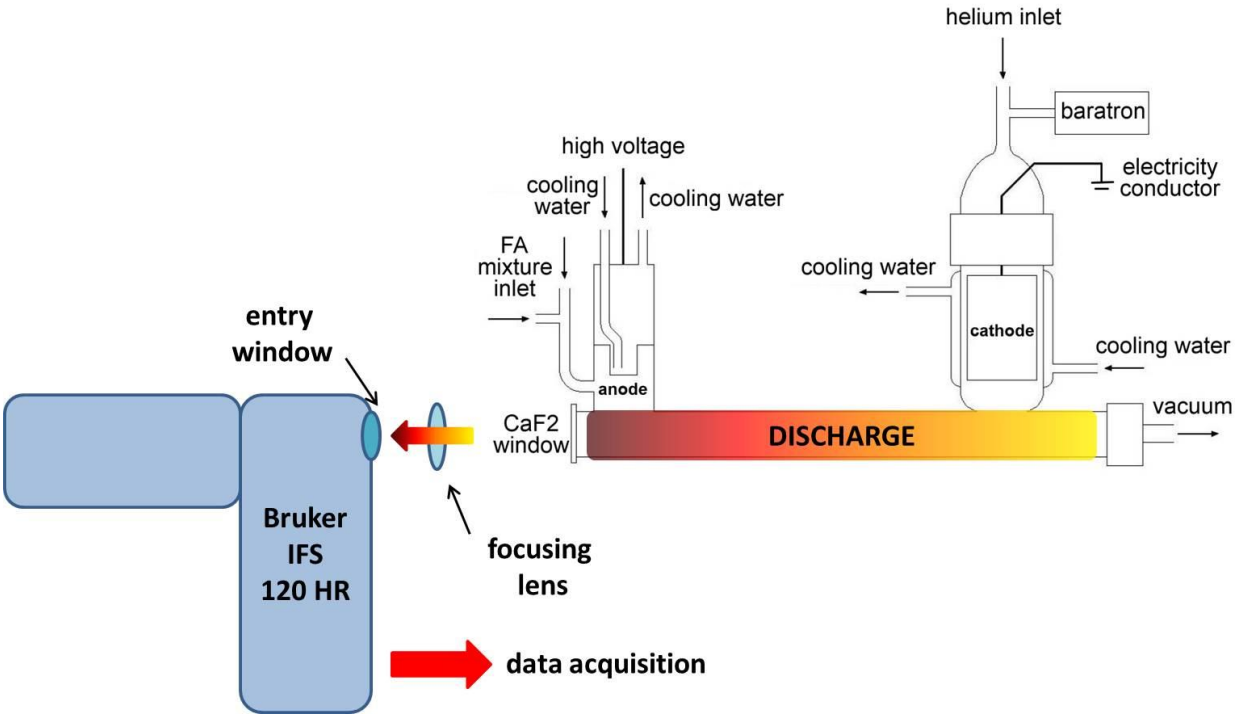

Figure 1: Scheme of experimental arrangement

Because of the use of both MCT and InSb detectors, it was possible to record spectra in the range of 700-7000 cm^{-1}. The spectra were calibrated against precise line positions of fundamental and overtone CO bands in Guelachvili & Rao (1986).[56]

The time resolution played a role of adjusting the data output in accordance with the best possible signal-to-noise ratio in our experiments. The pulse width used was 22 μs, offset (time offset creates a dead time segment located before the data acquisition, for which the data acquisition is omitted) was 0-3 μs, mirror speed during measurement was 10 kHz, number of AD (acquisition of data) points was 30 and the sampling took place at each 3 μs.

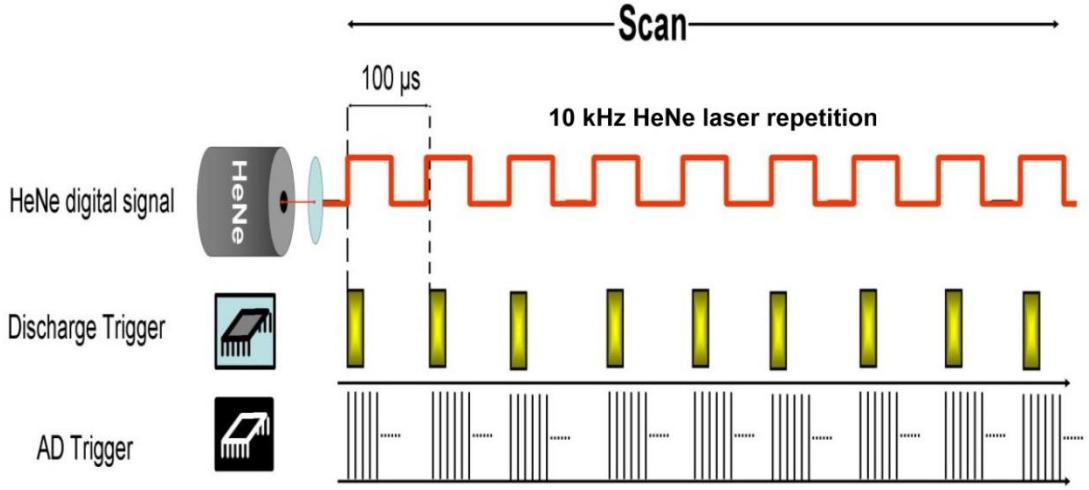

Figure 2: Scheme of time resolution (pairing with data acquisition)[57]

In Figure 2 it is possible to observe the data acquisition, paired with discharge trigger and HeNe digital tracing signal. When the mobile mirror speed is set to 10 kHz, one HeNe digital wave lasts 100 μs. At the beginning of the HeNe wave, the discharge pulse is placed. The pulse lasts for some time (in our experiments 22 μs) and with or without offset, data acquisition with defined parameters is started. In our experiments, data acquisition started with 0-3 μs offset and because there were 30 AD points at each 3 μs, the pulse was therefore observed in its beginning, duration and after its end as well. Such time resolution allowed us to pick only the best spectra for further analysis and therefore increase the signal-to-noise ratio even more.

Results and discussion

Table S1 in Supplementary Information file demonstrates the line list of the measured fundamental CO lines ($\Delta v = 1$), containing wavenumbers, line transition specifications (*J* and

v numbers, where the number marked with an apostrophe (‘) means an upper state, while the number marked with a quotation mark (“) means a lower state) and observed-calculated parameter (O-C), which presents information about the deduction of line positions calculated from Dunham fitting of all lines from experimental values. The data in Table S1 are sorted according to *v* number transitions from lowest (1-0) to highest (30-29). Within each *v*-transition, the data are also sorted by wavenumber.

Table S2 in Supplementary Information file presents a line list of CO’s first overtone (Δv = 2). The table copies the format style of Table S1.

Table 1 below demonstrates the Dunham coefficients that were obtained by Dunham fitting of all our experimental lines of fundamental and overtone CO bands. The total number of transitions involved in the fitting procedure was 2318. The table also shows the comparison of our data with data of other authors, sorted chronologically. The fitting procedure was performed according to well-known equation (1), describing the vibrational-rotational energy level of a diatomic molecule in the ground electronic state.

$$E_{vJ} = \sum_{mj} Y_{mj} \left(V + \frac{1}{2}\right)^{m} [J(J+1)]^{j} \qquad (1)$$

Where *E* stands for energy, *v* and *J* are vibrational and rotational quantum numbers and Y is Dunham parameter. 3 iteration cycles were used for the fitting procedure and an average deviation of 0.00187 cm^{-1} was achieved.

Table 1: Dunham parameters obtained from line fitting

Parameter	Our value	Deviation	Guelachvili 1983[2]	Farrenq 1991[13]	George 1994[12]	Voitsekhovskaya 2010[21]	Velichko 2012[37]
Y_{10}	2.16981435058E+03	2.60346E-04	2.169813079E+03	2.169812670E+03	2.1698127220761E+03	2.16981260189138E+03	2.16981271269893E+03
Y_{20}	-1.32880451734E+01	6.90001E-05	-1.328790597E+01	-1.328787634E+01	-1.3287915708423E+01	-1.32880390472301E+01	-1.32879077503162E+01
Y_{30}	1.04196903414E-02	8.31465E-06	1.041444739E-02	1.041106647E-02	1.0423331951946E-02	1.04297230421766E-02	1.04200107689629E-02
Y_{40}	6.92027520078E-05	4.61776E-07	6.921598529E-05	6.936640756E-05	6.7462405343680E-05	6.91624678098570E-05	6.80377742384337E-05
Y_{50}	1.68790806557E-07	1.02696E-08	1.657890319E-07	1.679352306E-07	3.2986711937998E-07	-	2.78361050612498E-07
Y_{60}	2.05925160000E-09	fixed*	2.466226718E-09	2.059251576E-09	-5.8493637376180E-09	-	-3.19724526593943E-09
Y_{70}	-8.48735465211E-10	2.05532E-12	-8.630071431E-10	-8.488145707E-10	-6.2715847364920E-10	-	-7.06823058539760E-10
Y_{80}	1.23977200000E-11	fixed*	1.261536024E-11	1.239772013E-11	9.0775889392701E-12	-	1.03749356544423E-11
Y_{90}	-8.23373730000E-14	fixed*	-8.363842545E-14	-8.233737278E-14	-6.1705367158987E-14	-	-7.05404492531844E-14
Y_{01}	1.93128382294E+00	3.06305E-06	1.931280862E+00	1.931280985E+00	1.9312809033958E+00	1.93128401690855E+00	1.93128087327140E+00
Y_{11}	-1.75043277315E-02	3.18138E-07	-1.750410155E-02	-1.750439229E-02	-1.7504193371413E-02	-1.75116889793261E-02	-1.75041235527725E-02
Y_{21}	7.41356432756E-07	2.75631E-08	5.422101371E-07	7.173917007E-07	6.2379766846640E-07	1.92588311032083E-06	5.70532184909572E-07
Y_{31}	-2.26621471569E-08	6.82024E-10	1.311844382E-08	-2.146354586E-08	-7.0546494085138E-09	-1.40220011143880E-07	9.69857903930996E-09
Y_{41}	4.43540390000E-09	fixed*	1.401093703E-09	4.435403909E-09	3.4920931173138E-09	4.34781878468765E-09	1.35483542867397E-09
Y_{51}	-1.36106950000E-10	fixed*	-5.829907475E-12	-1.361069450E-10	-1.0881270072104E-10	-	2.25449888217700E-11
Y_{61}	1.24578570000E-12	fixed*	-1.434127145E-12	1.245785715E-12	9.5370204560962E-13	-	-3.19275246504171E-12
Y_{71}	-2.12512340000E-14	fixed*	-	-2.125123415E-14	-2.1251311385081E-14	-	4.32011471696302E-14
Y_{02}	-6.12311794934E-06	2.43250E-09	-6.120747566E-06	-6.121615183E-06	-6.1215848016203E-06	6.13285831240000E-06	-6.12158560096097E-06
Y_{12}	1.03492300000E-09	fixed*	9.449843095E-10	1.034922952E-09	1.0188484060611E-09	-1.01342795667900E-08	1.02459633331244E-09
Y_{22}	-1.84976700000E-10	fixed*	-1.450768382E-10	-1.849766981E-10	-1.8203310242138E-10	1.91114139748080E-09	-1.80717504333141E-10
Y_{32}	2.43111090000E-12	fixed*	-2.927592559E-12	2.431110877E-12	1.7737257777330E-12	-1.55862557242420E-10	1.22972770958921E-12
Y_{42}	-1.04348860000E-13	fixed*	1.660533203E-13	-1.043488564E-13	-1.0434878309722E-13	1.23163810413664E-12	-4.92314710035746E-15
Y_{03}	5.88490500000E-12	fixed*	5.555386989E-12	5.884905033E-12	5.8860382897684E-12	7.49718003847800E-12	5.88575750614083E-12
Y_{13}	-1.42865330000E-13	fixed*	-1.512463732E-13	-1.428653277E-13	-1.4336331475578E-13	4.39367271266751E-13	-1.43834090220217E-13
Y_{23}	-1.22532850000E-15	fixed*	-1.471295100E-15	-1.225328499E-15	-1.0421817812590E-15	-4.13264102453580E-13	-7.89546451928477E-16
Y_{04}	-3.61578570000E-17	fixed*	-	-3.615785745E-17	-3.6175232747399E-17	-	-3.61692680681491E-17
Y_{14}	-7.40580130000E-19	fixed*	-	-7.405801298E-19	-7.2671020958070E-19	-	-7.18415798732584E-19
Y_{24}	-5.05437660000E-21	fixed*	-	-5.054376594E-21	-5.0546748483490E-21	-	-9.48909588925019E-21
Y_{05}	-4.55529850000E-23	fixed*	-	-4.555298526E-23	-4.5798771172546E-23	-	-4.60743885881130E-23
Y_{15}	-5.92225750000E-24	fixed*	-	-5.922257515E-24	-5.9223569597228E-24	-	-4.99321091850083E-24
Y_{06}	-1.51964150000E-27	fixed*	-	-1.519641502E-27	-1.5196377524508E-27	-	-7.78104388574249E-28

*In Table 1, column Deviation, fixed values represent Dunham coefficients, which were fixed at a constant value during fitting procedure. The values of such constants were always taken from Farrenq *et al*. (1991).[13] The table also does not contain all Dunham parameters found in selected literature, since not every parameter was used in the fitting procedure (see publications highlighted in Table 1 for the complete information).

Figure 3 presents the dependence of deviation (O-C, described in Table S1 and S2), obtained during Dunham fitting, of all lines of fundamental and overtone CO band on increasing wavenumber.

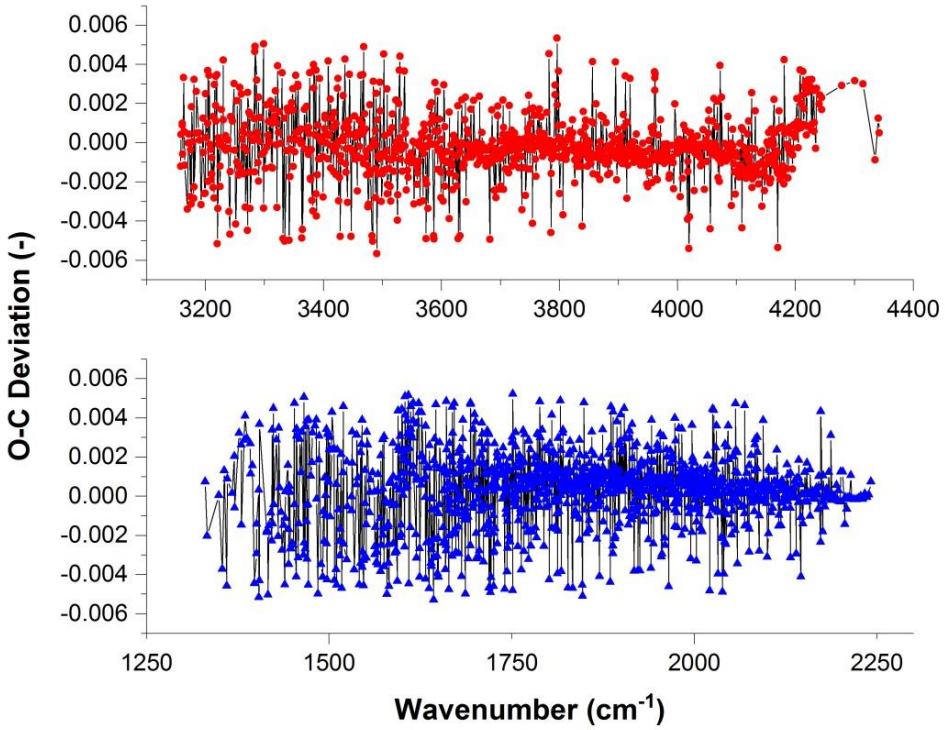

Figure 3: upper – O-C dependence on wavenumber for CO overtone band
lower – O-C dependence on wavenumber for CO fundamental band

In an ideal case, Figure 3 should demonstrate a random distribution of deviations, which should not deviate from zero extremely. From Figure 3, it is obvious the deviation distribution of overtone and also fundamental lines is almost ideally random. However, it can be noticed that deviations of CO overtone contain some residuals mainly in 4200-4400 cm^{-1} region.

Figure 4 below demonstrates the overall composition of whole fundamental and overtone CO bands at 33rd μs of the data acquisition.

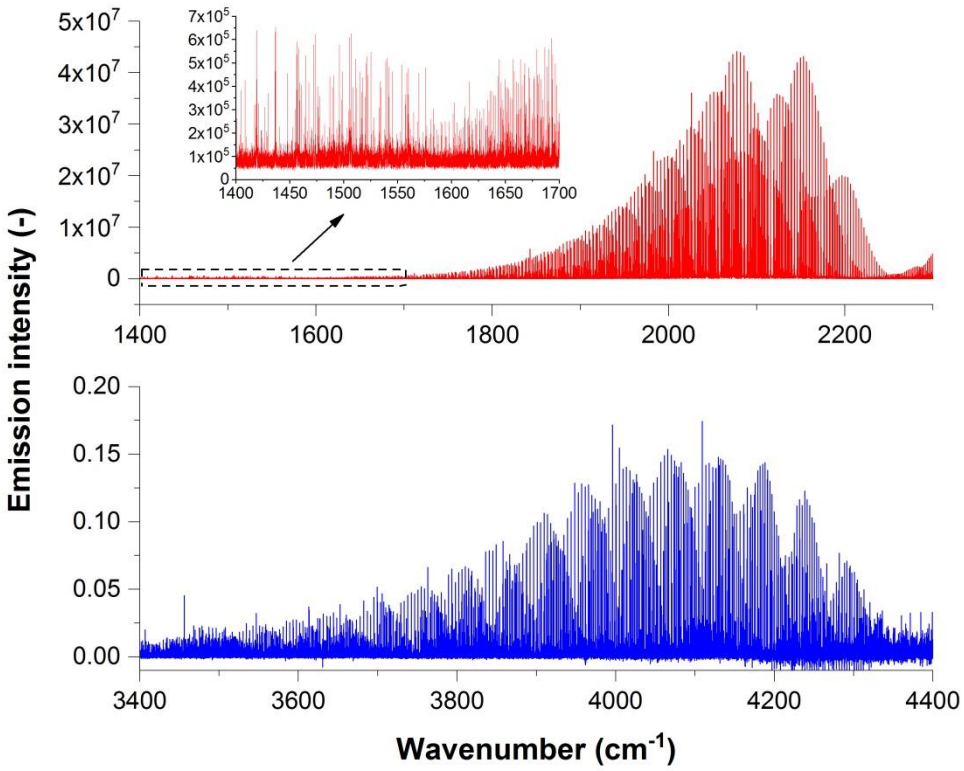

Figure 4: upper – fundamental CO band, lower – first overtone CO band (at 33 μs)

Figure 4 above was obtained by selecting only the most intense spectra from the matrix of time-resolved spectral set. A brief overview of such time-dependent spectral dataset can be observed in Figure 5 below.

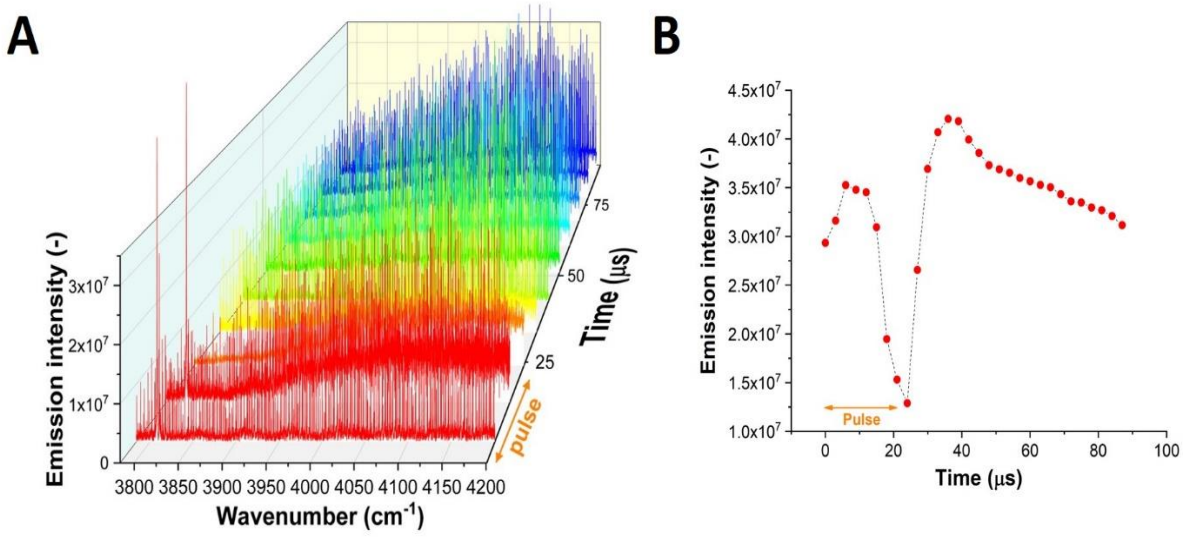

Figure 5: panel A – 3D model of time-resolved CO overtone spectra
panel B – selected time profile of any CO overtone line

It can be seen from panel B of Figure 5 that CO reaches the highest emission intensity at approximately 33 μs, which is 11 μs after the discharge pulse.

When a pure CO glow discharge is realised, almost no overtone band can be observed, which is an opposite situation to formamide-mixture discharge. This effect can be observed in Figure 6. Measurements summarized by Figure 5 were performed under the same stable conditions (1.8 torr of helium buffer gas, 0.2 torr of formamide-nitrogen-water mixture or 0.2 torr of pure carbon monoxide). The experimental setup of the IFS 120 HR spectrometer also remained the same.

d

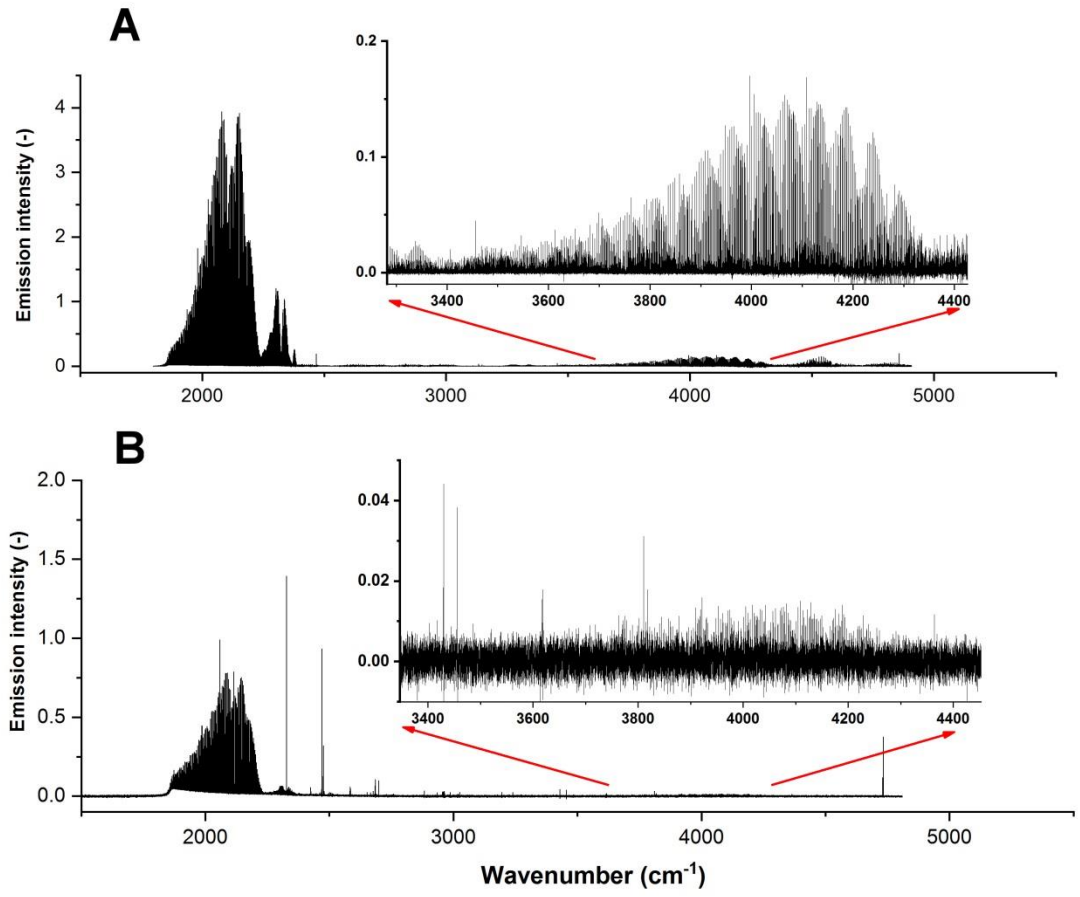

Figure 6: Comparison of formamide-mixture and pure CO discharge (33rd μs)
panel A – helium + formamide-mixture discharge
panel B – helium + pure CO discharge

As can be observed in Figure 6, formamide-mixture (helium, formamide vapour, water vapour, nitrogen) glow discharge produces both fundamental and overtone CO bands. On the other hand, pure CO mixed with helium as a buffer gas almost does not populate first

overtone CO band at all. This phenomenon is related to accessible excitation energy available in the discharge system. While performing the glow discharge in the formamide-mixture system, a large amount of energy is emitted and transferred via many short or long living radicals and other species, which leads to high population of other energy mediators like CN and CO radical in various energy levels, including highly excited ones. Therefore, it is possible to observe the CO overtone band very easily. Also, from Figure 4 and 6 it may be observed the CO overtone resembles itself in inverted population, very similar to lasers involving CO. In the formamide-mixture system, CO overtone thus has higher intensity of some higher vibrational transitions than lower ones (e.g. 6-4 transition is much more intense than 2-0).

Non-LTE spectrum of CO

The inversely populated discharge spectrum of CO shown in Fig. 4 exhibits strong non-LTE character (see also Ferus *et al*. (2011, 2017)).[45,47] Although the rotational populations are found to satisfy the Boltzmann equilibrium at slightly under the experimental temperature (the best fit was found to be with T = 400 K), due to its small relaxation time the vibrational excitations are dominated by highly excited vibrational populations which cannot be associated with the Boltzmann distribution. Indeed, the strongest $\Delta v = 2$ bands in Figure 4 correspond to $\Delta v = 6 - 4$ (see Figure 7), while Boltzmann always assumes $v'' = 0$ to be the most populated. The intensities of the hot transitions are much higher than that of the fundamental ($1 \rightarrow 0$) or the overtone ($2 \rightarrow 0$), which otherwise would be dominating an LTE spectrum.

In our description of the dissociation processes leading to non-LTE vibrational population of the product is based on the structural differences between reactant and product assuming no significant change in nuclear configuration of the molecule following the polyatomic Franck-Condon type model by Band & Freed (1974)[58] and Berry (1974).[59] We also assume the following common approximations: (i) the dissociation processes that lead to the formation of the non-LTE CO gas happen instantaneously; (ii) only the vibrational ground state of the fragment is populated; (iii) that the modes for both the original molecule and the final fragment are completely separable, i.e. the internal vibration of the CO bond in formamide is decoupled from other modes; and (iv) the corresponding vibration of the CO-fragment and CO-product (diatomic) can be approximated by 1D harmonic oscillators. As such, the fragments bear the structural information of the molecule in the initial (or intermediate)

system owing to the relatively slow vibrational relaxation of the molecule.[44] For example, there are many routes of dissociation for formamide,[46,60,61] one of the routes leading to CO is via the structural configuration NH_2-C-O-H (structure INT-2b in Figure 7 in Nguyen *et al.* (2011))[60] with the corresponding equilibrium constants r_e = 1.335 Å and the harmonic constant ω_e = 1156 cm^{-1}.[60]

Following these assumptions, the corresponding CO vibrational wavefunctions (both fragment and product) are then approximated by a 1D Harmonic oscillator:

$$\Psi_v = C_v H_v(x) e^{\frac{-x^2}{2}}, \tag{2}$$

where

$$x = \frac{r - r_e}{\sqrt{\alpha}}, \tag{3}$$

$$\alpha = \sqrt{\frac{h}{4\pi^2 c \mu \omega_e}}, \tag{4}$$

μ is the reduced mass:

$$\frac{1}{\mu} = \frac{1}{m_C} + \frac{1}{m_O}, \tag{5}$$

h is the Planck constant, c is the speed of light, m_c is the nuclear mass of a carbon atom = 12.0000 Da, and m_o is the nuclear mass of an oxygen atom = 15.9949 Da.

The equilibrium parameters r_e and ω_e required for the description of the vibrational states of the free (gas phase) CO molecule are taken as the corresponding experimental values of 1.1283 Å and 2169.81358 cm^{-1},[62] respectively. Since the dissociative pathway to form CO from formamide is not well known, the corresponding equilibrium parameters r_e and ω_e of the CO fragment are treated as adjustable parameters. Their values are determined by adjusting the shape of the Δv = 1 and Δv = 2 bands of CO. The best values corresponding to the simulated spectrum shown in Figs. 6-8 and are r_e = 1.218 Å and ω_e = 1000 cm^{-1}, which, under the assumption of the instantaneous dissociation process, can be considered as an indication of the dissociation pathway. The corresponding parameters of the main isomer of formamide are r_e = 1.219 Å[63] and ω_e = 1618 cm^{-1}.[60]

The vibrational populations of the product CO are then estimated from the Franck-Condon factors $\langle v'' = 0(\text{fragment})|v'(\text{gas phase})\rangle$ i.e. overlap integrals between the fragment wavefunction $|v''\rangle$ (which is assumed to be in its ground vibrational state) and the gas phase CO wavefunctions $|v'\rangle$ ($v' = 0 \leq x \leq 30$):

$$N_v^{\text{vib}} = \langle 0(\text{fragment})|v(\text{g. ph.})\rangle^2, \tag{6}$$

where N_v^{vib} are the population densities for each vibrational energy level of the gas phase of CO. The calculated populations N_v^{vib} were then combined with the ExoMol line list to give a weighting for all transitions in the CO line list calculated by Li *et al*. in 2015.[54] This is done by incorporating the non-LTE vibrational densities into the ExoMol States file (the ExoMol file formats are discussed extensively elsewhere).[55] The non-LTE spectrum of CO for a given *T* and *P* are then calculated using the Einstein-A coefficients by Li *et al*. (2015)[54] as provided by ExoMol (www.exomol.com) with the ExoCross program.[64] The rotational populations are assumed to be in LTE. The final ro-vibrational population is thus given by

$$N_{rv} = N_v^{\text{vib}}(2J+1)e^{\frac{-c_2\tilde{E}_J^{\text{rot}}}{T}}. \tag{7}$$

Here c_2 is the second radiation constant and $\tilde{E}_J^{\text{rot}}$ is the rotation contribution to $\tilde{E}_{J,v}$ (ro-vibrational energy term value) for a given vibrational state defined as

$$\tilde{E}_J^{\text{rot}} = \tilde{E}_{J,v} - \tilde{E}_v^{\text{vib}}. \tag{8}$$

Here we apply our 1D model to simulate the CO non-LTE features of the discharged formamide shown in Figure 4. The details of the model will be presented elsewhere.

The comparison between the calculated non-LTE spectra of CO and the experimental spectra for both the fundamental and first overtone CO band are shown in Figures 7 and 8, where we used r_e = 1.218 Å and ω_e = 1000 cm^{-1}, and calculate an absorption spectrum using the ExoCross program[64] with a rotational temperature of 400 K.

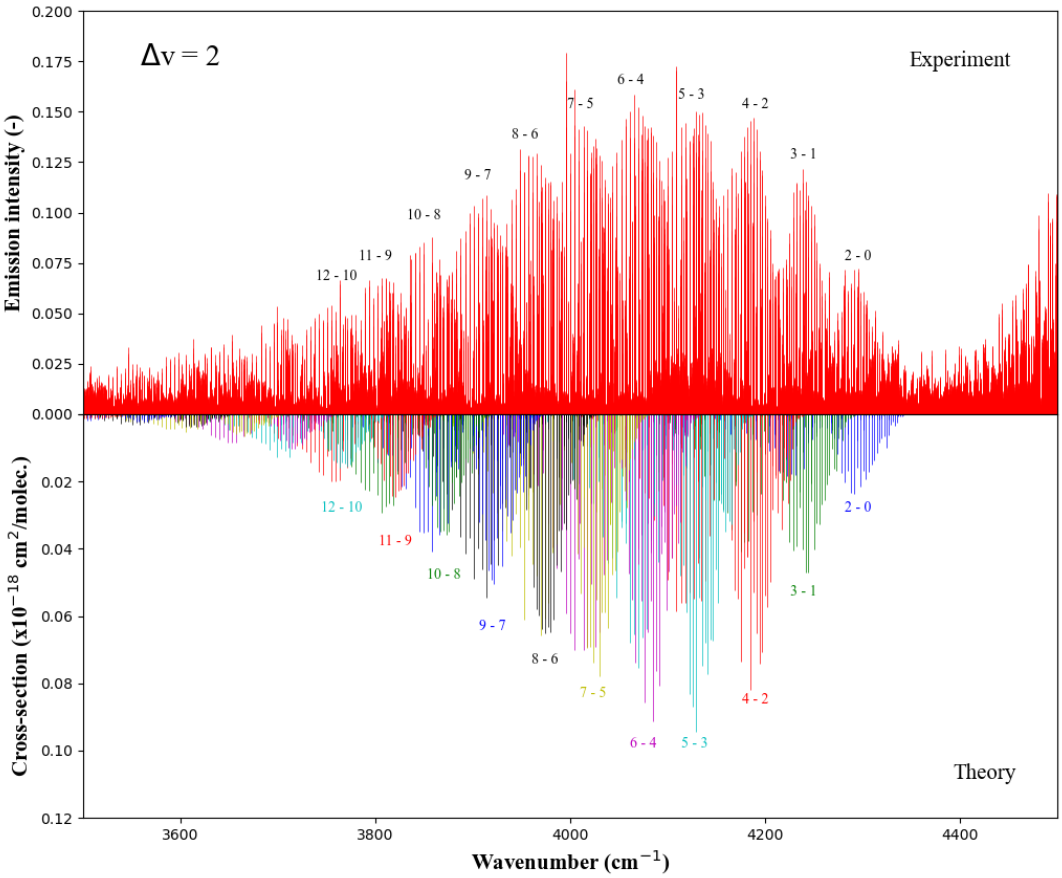

Figure 7: Comparison of the experimental (top) and theoretical (bottom) spectra for the $\Delta v = 2$ band of $^{12}C^{16}O$, from 3500 cm^{-1} to 4500 cm^{-1}

In Figure 7, the vibrational quantum numbers are labelled for both the experimental and theoretical spectra, with the theoretical spectrum containing transitions from Δv = 2-0 up to and including Δv = 17-15. Here and in Figure 8, we used the grid spacing of 0.03 cm^{-1}, a Voigt line profile of γ = 0.007 cm^{-1} and pressure of 1.0 bar.

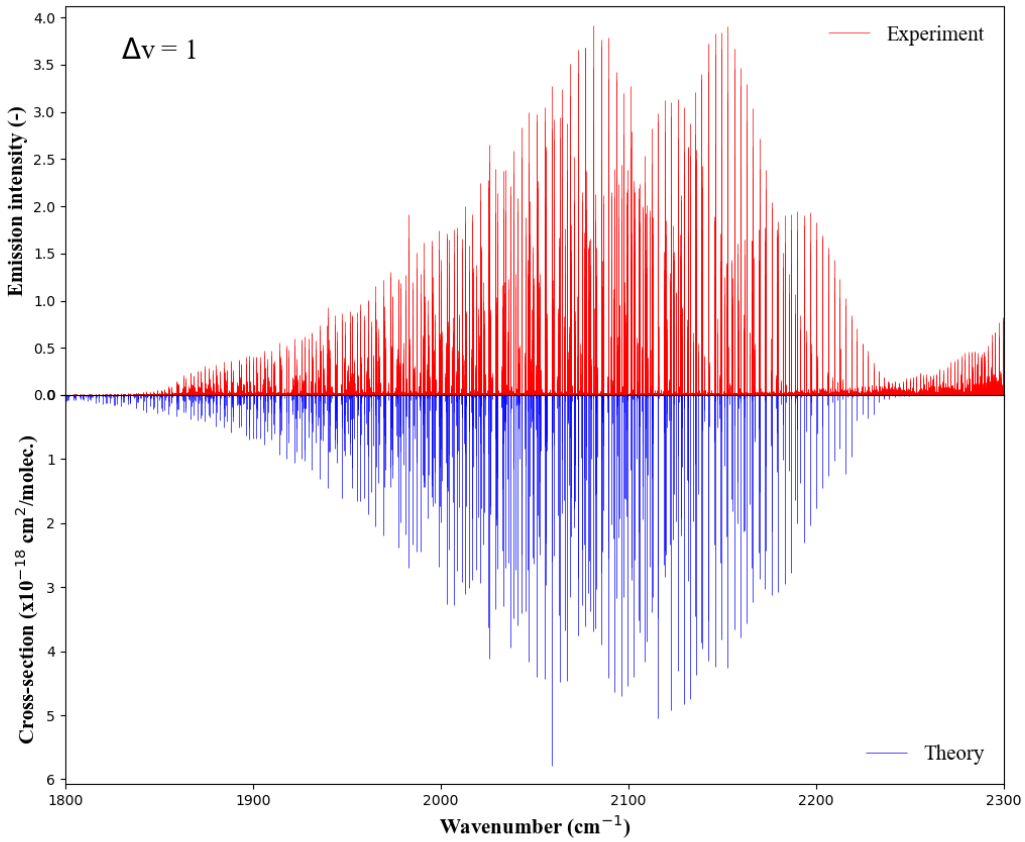

Figure 8: Comparison of the experimental (red) and theoretical (blue) spectra for the Δv = 1 band of $^{12}C^{16}O$, from 1800 cm^{-1} to 2300 cm^{-1}

It is clear to see that both the position and shape profile of the experimental and calculated peaks are in good agreement with each other, and the intensity profiles also agree, albeit the 4000 cm^{-1} peak is slightly weaker than experimental. The 'tails' of the curves also match well for both the Δv = 1 and Δv = 2 bands, with both spectra having the same non-Boltzmann, asymmetric distribution. Despite the good overall agreement, there are a few notable differences. The intensity of the experimental spectrum decreases suddenly at around 1850 cm^{-1} in the Δv = 1 peak which our calculated spectrum does not emulate, indicating that our model is less accurate in this region. We also see some differences in the fine structure, such as the intense experimental features in the Δv = 1 band at 1982.77 cm^{-1} and the Δv = 2 band at 3762.94 cm^{-1} which are not well reproduced by theory. However, similar strong experimental features in the Δv = 1 band at 2025.87 cm^{-1} and the Δv = 2 band at 3995.73 cm^{-1} are well described. The inability of our model to describe some of the fine structure can be attributed

to the simplified broadening model (Voigt with a fixed HWHM) used here. The additional sub-shoulders to the far right of both the 2000 cm^{-1} and the 4000 cm^{-1} peaks in the experimental spectra, which do not appear in the theoretical spectra, correspond to different species such as CO_2.[45]

Conclusion

In this publication we present an extension of carbon monoxide line list up to v = 30 for the fundamental CO band and up to v = 24 for the first CO overtone band, where all the data are within maximal J number equal to 30. Lines in the higher vibrational number transitions have not been experimentally measured before, but it has to be noted that others, especially Farrenq *et al.*,[13] have measured CO under high-temperature and therefore extended the available CO line list to higher J values (up to J = 110).

We also performed the Dunham fitting of both fundamental and overtone CO bands simultaneously and obtained Dunham parameters relevant to this fitting procedure.

Furthermore, we present a comparison between the glow discharge realized in formamide-nitrogen-water mixture and the glow discharge realized in pure CO under the same experimental conditions. It is possible to observe the CO first overtone is almost not populated in the pure CO discharge, which is caused by inaccessibility of suitable excitation energy in the discharge system. On the other hand, formamide-mixture discharge creates an inversely populated CO first overtone, which is a sign of abundance of energy mediators like CN and CO radicals in the system.

Lastly, we calculated the non-LTE spectrum for the fundamental and first overtone band of $^{12}C^{16}O$ using a 1D harmonic approximation and the CO ExoMol line list. Our comparison of the experimental and calculated spectra shows good agreement. We are planning to apply the non-LTE to simulate the complete non-LTE spectrum of the discharged formamide system along with a more detailed analysis of our non-LTE model. In case of three-atomic molecules, the 1D population model can be relatively straightforwardly extended to a full 3D treatment, which we have implemented in the variational program TROVE.[65] The description of the extended 3D non-LTE model and applications to the description of other discharged fragments of formamide will be published elsewhere.

Acknowledgements

This work was funded by grant no. CZ.02.1.01/0.0/0.0/16_019/0000778 alias “ERDF/ESF Centre of Advanced Applied Sciences”.

References

1. Guelachvili, G. Absolute wavenumbers and molecular constants of the fundamental bands of 12C16O, 12C17O, 12C18O, 13C16O, 13C17O, 13C18O and of the 2-1 bands of 12C16O and 13C16O, around 5µm, by Fourier spectroscopy under vacuum. *J. Mol. Spectrosc.* **75**, 251–269 (1979).

2. Guelachvili, G., de Villeneuve, D., Farrenq, R., Urban, W. & Verges, J. Dunham coefficients for seven isotopic species of CO. *J. Mol. Spectrosc.* **98**, 64–79 (1983).

3. Chen, D. W., Narahari Rao, K. & McDowell, R. S. Fundamental and overtone bands of isotopic species of carbon monoxide. *J. Mol. Spectrosc.* **61**, 71–78 (1976).

4. Whittet, D. C. B. & Duley, W. W. Carbon monoxide frosts in the interstellar medium. *Astron. Astrophys. Rev.* **2**, 167–189 (1991).

5. Lambert, D. L., Dearborn, D. S. & Sneden, C. The C-12/C-13 ratio in stellar atmospheres. II - CN and CO in alpha Orionis. *Astrophys. J.* **193**, 621 (1974).

6. Rank, D. M., Geballe, T. R. & Wollman, E. R. Detection of ^{17}O in IRC+10216. *Astrophys. J.* **187**, L111 (1974).

7. Hagen, W., Allamandola, L. J. & Greenberg, J. M. Infrared absorption lines by molecules in grain mantles. *Astron. Astrophys.* **86**, L3–L6 (1980).

8. Oka, T. & Geballe, T. R. The Central 300 pc of the Galaxy Probed by Infrared Spectra of H 3 + and CO. II. Expansion and Morphology of the Warm Diffuse Gas. *Astrophys. J.* **902**, 9 (2020).

9. Ogilvie, J. F., Cheah, S. L., Lee, Y. P. & Sauer, S. P. A. Infrared spectra of CO in absorption and evaluation of radial functions for potential energy and electric dipolar moment. *Theor. Chem. Acc.* **108**, 85–97 (2002).

10. Narahari Rao, K. *Wavelength Standards in the Infrared*. (Academic Press, 1966).

11. Gordon, I. E. *et al.* The HITRAN 2016 molecular spectroscopic database. *J. Quant. Spectrosc. Radiat. Transf.* **203**, 3–69 (2017).

12. George, T., Urban, W. & Lefloch, A. Improved mass-independent dunham parameters for the ground state of co and calibration frequencies for the fundamental band. *Journal of Molecular Spectroscopy* **165**, 500–505 (1994).

13. Farrenq, R., Guelachvili, G., Sauval, A. J., Grevesse, N. & Farmer, C. B. Improved Dunham coefficients for CO from infrared solar lines of high rotational excitation. *J. Mol. Spectrosc.* **149**, 375–390 (1991).

14. Varberg, T. D. & Evenson, K. M. Accurate far-infrared rotational frequencies of carbon monoxide. *Astrophys. J.* **385**, 763 (1992).

15. Gendriesch, R. *et al.* Accurate laboratory rest frequencies of vibrationally excited CO up to v = 3 and up to 2 THz. *Astron. Astrophys.* **497**, 927–930 (2009).

16. Todd, T. R., Clayton, C. M., Telfair, W. & Ubbin, T. K. M. Infrared Emission of 12C160 , 13C160 , and 12P01. (1976).

17. Klapper, G. *et al.* Laboratory Precision Measurements of the Rotational Spectrum of 12 C 17 O

and 13 C 17 O . *Astrophys. J.* **582**, 262–268 (2003).

18. Klapper, G., Lewen, F., Gendriesch, R., Belov, S. P. & Winnewisser, G. Sub-Doppler Measurements of the Rotational Spectrum of 13C16O. *J. Mol. Spectrosc.* **201**, 124–127 (2000).

19. Winnewisser, G., Belov, S. P., Klaus, T. & Schieder, R. Sub-Doppler Measurements on the Rotational Transitions of Carbon Monoxide. *J. Mol. Spectrosc.* **184**, 468–472 (1997).

20. Watson, J. K. G. The isotope dependence of diatomic Dunham coefficients. *J. Mol. Spectrosc.* **80**, 411–421 (1980).

21. Voitsekhovskaya, O. K., Kashirskii, D. E. & Korchikov, V. S. Determination of dunham coefficients and calculation of the energies of highly excited vibrational-rotational levels of the carbon monoxide molecule in the electronic ground state. *Moscow Univ. Phys. Bull.* **65**, 386–391 (2010).

22. Coxon, J. A. & Hajigeorgiou, P. G. Direct potential fit analysis of the X1Σ+ ground state of CO. *J. Chem. Phys.* **121**, 2992–3008 (2004).

23. Rytel, M. & Rytel, T. Dunham Series Coefficients up to 20th Order. *J. Mol. Spectrosc.* **185**, 417–419 (1997).

24. de Natale, P., Inguscio, M., Orza, C. R. & Zink, L. R. Far-infrared Fourier transform spectroscopy of (C-12)(0-18). *Astrophys. J.* **370**, L53 (1991).

25. Maki, A. G., Wells, J. S. & Jennings, D. A. Heterodyne frequency measurements of CO and OCS beyond 2100 cm-1. *J. Mol. Spectrosc.* **144**, 224–229 (1990).

26. Tyuterev, V. G. & Velichko, T. I. High-order anharmonicity parameters in various representations of the diatomic potential function and exact relations between spectroscopic constants. application to the co molecule. *Chem. Phys. Lett.* **104**, 596–604 (1984).

27. Rothman, L. S. *et al.* HITEMP, the high-temperature molecular spectroscopic database. *J. Quant. Spectrosc. Radiat. Transf.* **111**, 2139–2150 (2010).

28. Belov, S. P., Tret'iakov, M. I. & Suenram, R. D. Improved laboratory rest frequency measurements and pressure shift and broadening parameters for the J = 2 - 1 and J = 3 - 2 rotational transitions of CO. *Astrophys. J.* **393**, 848 (1992).

29. Yoshida, T. & Sasada, H. Near-infrared spectroscopy with a wavemeter. *J. Mol. Spectrosc.* **153**, 208–210 (1992).

30. Cazzoli, G., Puzzarini, C. & Lapinov, A. V. Precise Laboratory Frequencies for the J = 1-0 and J = 2-1 Rotational Transitions of C18O. *Astrophys. J.* **592**, L95–L98 (2003).

31. George, T., Wu, B., Dax, A., Schneider, M. & Urban, W. Saturation stabilization of the CO fundamental-band laser. *Appl. Phys. B Photophysics Laser Chem.* **53**, 330–332 (1991).

32. Malathy Devi, V., Benner, D. C., Smith, M. A. H. & Rinsland, C. P. Self-broadening and self-shift coefficients in the fundamental band of 12C16O. *J. Quant. Spectrosc. Radiat. Transf.* **60**, 815–824 (1998).

33. Wappelhorst, M. H. *et al.* Sub-doppler heterodyne frequency measurements on isotopic species of carbon monoxide and improved frequencies for secondary standards near 60 THz. *J. Mol. Spectrosc.* **181**, 357–362 (1997).

34. George, T., Saupe, S., Wappelhorst, M. H. & Urban, W. The CO fundamental-band laser as secondary frequency standard at 5 µm. *Appl. Phys. B Lasers Opt.* **59**, 159–166 (1994).

35. Rothman, L. S. *et al.* The HITRAN 2008 molecular spectroscopic database. *J. Quant. Spectrosc. Radiat. Transf.* **110**, 533–572 (2009).

36. Tashkun, S. A., Velichko, T. I. & Mikhailenko, S. N. Critical evaluation of measured pure-rotation and rotation-vibration line positions and an experimental dataset of energy levels of 12C16O in X1Σ+ state. *J. Quant. Spectrosc. Radiat. Transf.* **111**, 1106–1116 (2010).

37. Velichko, T. I., Mikhailenko, S. N. & Tashkun, S. A. Global Multi-isotopologue fit of measured rotation and vibration-rotation line positions of CO in X 1σ + state and new set of mass-independent Dunham coefficients. *J. Quant. Spectrosc. Radiat. Transf.* **113**, 1643–1655 (2012).

38. Mishra, A. P., Shetty, B. J. & Kshirsagar, R. J. Fourier transform emission spectroscopy of Δv = 2 sequence bands of the CO molecule in the ground electronic state. *J. Mol. Spectrosc.* **232**, 296–307 (2005).

39. Devi, V. M., Benner, D. C., Smith, M. A. H., Rinsland, C. P. & Mantz, A. W. Determination of self- and H2-broadening and shift coefficients in the 2-0 band of 12C16O using a multispectrum fitting procedure. *J. Quant. Spectrosc. Radiat. Transf.* **75**, 455–471 (2002).

40. Picqué, N. & Guelachvili, G. Absolute wavenumbers and self-induced pressure lineshift coefficients for the 3-0 vibration-rotation band of 12C16O. *J. Mol. Spectrosc.* **185**, 244–248 (1997).

41. Swann, W. C. & Gilbert, S. L. Pressure-induced shift and broadening of 1560–1630-nm carbon monoxide wavelength-calibration lines. *J. Opt. Soc. Am. B* **19**, 2461 (2002).

42. Chung, C. Y., Ogilvie, J. F. & Lee, Y. P. Detection of vibration-rotational band 5-0 of12C16O X 1∑+ with cavity ringdown absorption near 0.96 µm. *J. Phys. Chem. A* **109**, 7854–7858 (2005).

43. Civiš, S., Šedivcová-Uhlíková, T., Kubelík, P. & Kawaguchi, K. Time-resolved Fourier transform emission spectroscopy of A2Π-X2Σ+ infrared transition of the CN radical. *J. Mol. Spectrosc.* **250**, 20–26 (2008).

44. Dudás, E. *et al.* Higherature hypersonic Laval nozzle for non-LTE cavity ringdown spectroscopy. *J. Chem. Phys.* **152**, (2020).

45. Ferus, M. *et al.* HNC/HCN ratio in acetonitrile, formamide, and BrCN discharge. *J. Phys. Chem. A* **115**, 1885–1899 (2011).

46. Ferus, M. *et al.* High-Energy Chemistry of Formamide: A Simpler Way for Nucleobase Formatione. *J. Phys. Chem.* **118**, 719–736 (2014).

47. Ferus, M. *et al.* High Energy Radical Chemistry Formation of HCN-rich Atmospheres on early Earth. *Sci. Rep.* **7**, Article number: 6275 (2017).

48. Pannier, E. & Laux, C. O. RADIS: A nonequilibrium line-by-line radiative code for CO2 and HITRAN-like database species. *J. Quant. Spectrosc. Radiat. Transf.* **222**–**223**, 12–25 (2019).

49. Campbell, D. H. & Muntz, E. P. Non-Boltzmann, non-Treanor vibrational level populations of electrical discharge excited nitrogen. *J. Chem. Phys.* **72**, 1487–1498 (1980).

50. Aliat, A., Kustova, E. V. & Chikhaoui, A. State-to-state reaction rates in gases with vibration-electronic- dissociation coupling: The influence on a radiative shock heated CO flow. *Chem.*

Phys. **314**, 37–47 (2005).

51. Macdonald, R., Munafò, A., Johnston, C. O. & Panesi, M. State-to-state modeling of CO for mars entry applications. *53rd AIAA Aerosp. Sci. Meet.* 1–12 (2015). doi:10.2514/6.2015-0476

52. Sahai, A., Lopez, B. E., Johnston, C. O. & Panesi, M. Novel approach for CO2 state-to-state modeling and application to multi-dimensional entry flows. *AIAA SciTech Forum - 55th AIAA Aerosp. Sci. Meet.* 1–19 (2017). doi:10.2514/6.2017-0213

53. Singh, N. & Schwartzentruber, T. Non-Boltzmann vibrational energy distributions and coupling to dissociation rate. *J. Chem. Phys.* **152**, 224301 (2020).

54. Li, G. *et al.* Rovibrational line lists for nine isotopologues of the co molecule in the X 1σ+ ground electronic state. *Astrophys. Journal, Suppl. Ser.* **216**, (2015).

55. Tennyson, J. *et al.* The 2020 release of the ExoMol database: Molecular line lists for exoplanet and other hot atmospheres. *J. Quant. Spectrosc. Radiat. Transf.* **255**, (2020).

56. Guelachvili, G. & Narahari Rao, K. *Handbook of infrared standards*. (ACADEMIC PRESS INC. LTD., 1986).

57. Kawaguchi, K., Baskakov, O., Hosaki, Y., Hama, Y. & Kugimiya, C. Time-resolved Fourier transform spectroscopy of pulsed discharge products. *Chem. Phys. Lett.* **369**, 293–298 (2003).

58. Band, Y. B. & Freed, K. F. Dissociation processes of polyatomic molecules. *J. Chem. Phys.* **63**, 3382–3397 (1975).

59. Berry, M. J. Golden rule calculation of reaction product vibronic state distributions. *Chem. Phys. Lett.* **27**, 73–77 (1974).

60. Nguyen, V. S. *et al.* Theoretical Study of Formamide Decomposition Pathways. *J. Phys. Chem. A* **115**, 841–851 (2011).

61. Ferus, M. *et al.* On the Road from Formamide Ices to Nucleobases: IR-Spectroscopic Observation of a Direct Reaction between Cyano Radicals and Formamide in a High-Energy Impact Event. *J. Am. Chem. Soc.* **134**, 20788–20796 (2012).

62. Huber, K. P. & Herzberg, G. H. Constants of Diatomic Molecules. *NIST Chemistry WebBook* doi:10.18434/T4D303

63. Hirota, E., Sugisaki, R., Nielsen, C. J. & Sørensen, G. O. Molecular structure and internal motion of formamide from microwave spectrum. *J. Mol. Spectrosc.* **49**, 251–267 (1974).

64. Yurchenko, S. N., Al-Refaie, A. F. & Tennyson, J. ExoCross: A general program for generating spectra from molecular line lists. *arXiv* **131**, 1–12 (2018).

65. Yurchenko, S. N., Thiel, W. & Jensen, P. Theoretical ROVibrational Energies (TROVE): A robust numerical approach to the calculation of rovibrational energies for polyatomic molecules. *J. Mol. Spectrosc.* **245**, 126–140 (2007).